ELSEVIER

International Journal of Mass Spectrometry 219 (2002) 429–443

International Journal of Mass Spectrometry

www.elsevier.com/locate/ijms

Experimental and theoretical studies on the gas phase reactivity of formamide–Ni^+ complexes generated by FAB and electrospray ionization

L. Rodríguez-Santiago[1], J. Tortajada*

Laboratoire Analyse et Environnement, CNRS UMR CNRS 8587, Université d'Evry-Val-d'Essonne, Bât. des Sciences, Boulevard François Mitterrand, F-91025 Evry Cedex, France

Received 27 December 2001; accepted 28 March 2002

Dedicated to our colleague and friend, Yannik Hoppilliard, on the occasion of her 60th birthday.

Abstract

The reactions between Ni^+ and formamide have been investigated by means of mass spectrometry experiments and theoretical methods. The [Ni–formamide]$^+$ adduct ions were generated by the CI-FAB and electrospray methods. The structure of several coordinated species corresponding to the metal cation interacting with formamide have been determined at the B3LYP DFT level. Calculations show that the most stable structure corresponds to the interaction of Ni^+ with the oxygen atom of formamide in *trans* position with respect to the amino group. The MIKE and ESI-CID spectra of [Ni–fomamide]$^+$ complex have been analyzed and show that this adduct ion undergoes fragmentation by different pathways depending on the used technique. The major fragmentation with both techniques corresponds to the dissociation into Ni^+ + formamide. The MIKE spectrum shows also important loss of NH_3. However, the ESI-CID low energy spectrum shows the loss of CO. In order to account for these differences of reactivity, several possible reaction channels leading to these fragmentations, and others ones (loss of H_2O, NCH), observed in a minor extend, have been studied at the B3LYP level. (Int J Mass Spectrom 219 (2002) 429–443)

Keywords: Gas phase; Formamide; Nickle(I) complexes; FAB; Electrospray; DFT; Ab initio calculation

1. Introduction

Over the past years there has been a growing interest in the study of the interactions between transition metal cations and relevant biological molecules due to the importance of these systems in several fields [1–3]. For example, it is well known that metal cations may interact with nucleic acids [4–9]. In general, metal cations interact with the phosphate groups of the nucleic acids, but transition metal cations possess significant affinities to nucleobases and are involved in several important biological processes [7,9]. Binding of a metal ion to the nucleobase can interfere into base pair interactions leading to a destabilization of the helix or to erroneous pairing. Several studies have been devoted to the interactions of nucleic acids bases with metal cations, both theoretically and experimentally [10].

* Corresponding author.
E-mail: jeanine.tortajada@chimie.univ-evry.fr
[1] Present address: Departament de Química, Universitat Autònoma de Barcelona, Bellaterra 08193, Barcelona.

1387-3806/02/$ – see front matter
PII S1387-3806(02)00698-X

On the other hand, many fundamental biological processes, such as oxygen transport, electron transfer or oxidation of target compounds need the presence of transition metal cations [11]. In these processes the active sites of the enzymes involve the interaction of the transition metal cation with one ore more amino acid residues. In addition, cationization with metal cations is becoming a useful tool to investigate the amino acid sequence of peptides in mass spectrometry experiments [12–14].

Mass spectrometry techniques can be used not only to determine gas-phase binding energies of neutral molecules to metal ions, but also to investigate the reactions induced by the metal cation. Metal cation complexation can induce the activation of some bonds of the neutral molecule. Thus, under mass spectrometry experiments, the spontaneous fragmentations or collision-induced dissociation (CID) processes of the ion–neutral molecule can be observed. When transition metal cations are used, the interactions with the neutral molecule are more specific, thus specific fragmentations can provide useful information on structure of the neutral molecule. The observed fragmentations can also provide information on the bonding and on some features of the potential energy surface (PES) of the complex. In this respect, the formation and fragmentation of complexes, such as transition metal cation–amino acid complexes have been studied by means of mass spectrometry techniques [15–26].

Formamide is a bidentate base and is the simplest amide containing a prototype HNC=O peptide linkage. Thus, it can be used as a model for the study of the hydrolysis of peptide bonds in living systems. Furthermore, formamide is also the simplest prototype that we can use to model the cationization of larger bases, in particular nucleobases like uracil, cytosine or thymine. In this way, formamide is a suitable model to study the reactivity of larger biochemical compounds, whose theoretical treatment is difficult and very time demanding due to their size.

Our group has been interested in recent years in the study of this kind of reactions. In previous studies we have focused our attention in the interaction of formamide with Li^+, Na^+, Mg^+ and Al^+ [27], Cu^+ [28] and Ag^+ [29]. To our knowledge, nobody has considered the interaction of Ni^+ with formamide. The Ni^+ cation is an open shell system with a d^9 (^2D) ground state, which plays an important role in some biological processes. Recently, we have reported a combined theoretical and experimental approach, to elucidate the glycine + Ni^+ interaction [26].

The aim of this paper is to investigate the gas-phase reactions between Ni^+ and formamide by means of mass spectrometry experiments and theoretical calculations. We will first discuss the formation and the unimolecular decomposition process of $[Ni–formamide]^+$ by means of mass-analyzed ionic kinetic energy spectroscopy (MIKES) [30]. The $[Ni–formamide]^+$ ion was generated first in a chemical ionization-fast atom bombardment ion source (CI-FAB). The recorded MIKE spectrum shows that $[Ni–formamide]^+$ complex undergoes fragmentation and leads mainly to the loss of formamide and NH_3.

We have also carried out experiments using an electrospray triple–quadrupole mass spectrometer. We have recorded MS/MS CID spectra of the $[Ni–formamide]^+$ complex formed in the electrospray source. In this case, the most important fragmentation corresponds to the elimination of formamide and CO, showing a different behavior with the CI-FAB mass spectrometry experiments. The rationalization of these experimental features can be tackled by a reliable description of the PES of the system in terms of local minima and transition states connecting them. Thus, we have studied theoretically the possible modes of coordination of Ni^+ to formamide and the possible pathways of the decomposition that lead to the experimentally observed fragment ions. Energies, geometries and vibrational frequencies of the different investigated species have been determined using the B3LYP density functional method.

2. Experimental

2.1. FAB experiments

The FAB mass spectrometric measurements were recorded on a double-focusing ZAB-HSQ mass

spectrometer (VG Analytical) of BEqQ configuration [31] (*B* and *E* represent the magnetic and electric sectors, *q* is a collision cell consisting of a rf-only quadrupole, and *Q* is a mass selective quadrupole). Complexes were generated by the CI-FAB method. The CI-FAB source was constructed from VG Analytical EI/CI and FAB ion source parts with the same modifications described by Freas et al. [32]. In that source the conventional FAB probe tip has been replaced by a foil of an alloy of chromium and nickel. "Naked" metal ions Cr^+ and Ni^+ were generated by bombarding this target with fast xenon atoms (Xe gas 7–8 keV kinetic energy, 1–2 mA of emission current in the FAB gun). Using alloys allows producing, at the same time, different metal cations.

The organic samples were introduced via a heated inlet system at 100 °C in a non-heated source. As mentioned by Schwarz and coworkers [33] we can assume that due to the relatively high pressure in the ion source (10^{-2} to 10^{-3} Pa), efficient collisional cooling of the ions takes place and therefore excited states of the Ni^+ ions are not likely to participate in the observed reactivity. The metal ion adduct complexes formed with formamide were mass selected (using an acceleration voltage of 8 kV) with the magnetic analyzer B metastable dissociations occurring in the second field-free region (2nd FFR) between the magnetic and the electric analyzers were monitored by scanning the later one. The metastable ion reactions were studied by MIKES techniques. The MIKE spectra were recorded at a resolving power of ∼1000.

2.2. Electrospray experiments

Electrospray mass spectra were recorded on an Applera/MDS Sciex API2000 triple–quadrupole instrument fitted with a "turboionspray" ion source. Samples were introduced in the source using direct infusion with a syringe pump at a flow rate of 5 μL/min. Ionization of the samples was achieved by applying a voltage of 5.5 kV on the sprayer probe and by using a nebulizing gas (GAS1, N_2), surrounding the sprayer probe, intersected by a heated gas (GAS2, N_2) at an angle of approximately 90°. The operating pressure of these two gases were typically 2.1 and 3.1 bar, respectively and the temperature of GAS2 was set at 100 °C. The curtain gas (N_2), which prevents air or solvent from entering the analyzer region, was adjusted at a pressure of 2.1 bar. As detailed in the following sections, the declustering potential (DP), defined as the potential difference between the orifice plate and the skimmer, was fixed to 60 V to record low-energy CID spectra. These MS/MS experiments were carried out by introducing nitrogen as collision gas in the second quadrupole, at a total pressure of 2×10^{-5} mbar, the background pressure being around 10^{-5} mbar. Collision energy settings ranging from 5 to 45 eV were done to follow the energy dependence of the CID spectra when varying the kinetic energy in the collision cell.

$[Ni–formamide]^+$ complexes were formed from a $NiSO_4$/formamide mixture in a water solution with concentrations of 10^{-4} and 5×10^{-4} mol/L, respectively. Source parameters were adjusted so as to optimize $[Ni–formamide]^+$ ion signal. ^{15}N labeling experiments were also performed. Formamide, ^{15}N labeled formamide and the $NiSO_4{\cdot}6H_2O$ metallic salts were purchased from Aldrich and used without further purification.

3. Computational details

Full geometry optimizations and harmonic vibrational frequency calculations of the different species under consideration have been performed using the non-local three parameter hybrid exchange B3LYP density functional method [34]. In order to identify the minima connected by a given transition state we have carried out intrinsic reaction coordinate (IRC) calculations at the same level of theory. The B3LYP method has been found to be quite reliable as far as the description of many transition metal-containing systems [35–39]. In particular, the adequacy of this method for the study of different metal cation–ligand systems has been shown in several papers [28,40–44]. For several small compounds, the B3LYP method has been shown to provide metal cation affinities that are in good agreement with experimental data [45,46].

Recently, Luna et al. [47] have studied a wide set of small systems using CCSD(T), B3LYP and G2-based methods. They have found that while G2 and the G2(MP2) methods to fail dramatically when trying to reproduce Cu^+ binding energies, the B3LYP method yields Cu^+ binding energies in fairly good agreement with the experimental values. Previous studies on metal cation–glycine systems [43,48], have shown that the B3LYP bond energies reproduce reasonably well the CCSD(T) ones. On the other hand, the B3LYP method has been applied successfully to the study of the [Cu–formamide]$^+$ system [28]. In a recent work devoted to $Ni^+ + C_3H_8$ reaction, Weisshaar and coworkers [49] suggested that B3LYP might overestimate some reaction barriers and specially when multicenter transition states are involved.

However, in order to establish the reliability of the B3LYP results for the [Ni–formamide]$^+$ system we have performed single point calculations using the single and double coupled cluster method with a perturbational estimate of the triple excitations CCSD(T) at the B3LYP geometries. In these calculations all valence electrons have been correlated.

Geometry optimizations and frequency calculations have been performed using the following basis set. The Ni basis set is a [8s 4p 3d] contraction of the (14s 9p 5d) primitive set of Wachters [50] supplemented with two diffuse p and one diffuse d function [51]. The final basis set is of the form (14s 11p 6d)/[8s 6p 4d]. The C, N and O basis set is the (9s 5p)/[4s 2p] set developed by Dunning [52], supplemented with one d polarization function ($\alpha = 0.75$ for carbon, $\alpha = 0.80$ for nitrogen and $\alpha = 0.85$ for oxygen). For H the basis set is the (4s)/[2s] set of Dunning [52], supplemented with a p polarization function. This basis set is referred to as D95(d,p) in the Gaussian 98 program [53]. Hereafter, this basis set will be referred as basis1.

Single point calculations at the B3LYP and CCSD(T) levels have been carried out using a larger basis set. The Ni basis set is augmented by a single contracted set of f polarization functions based on a three term fit to a Slater type orbital [54], which leads to a (14s 11p 6d 3f)/[8s 6p 4d 1f] basis set. This enlarged basis set for the metal is combined with the 6-311+G(3df, 2p) one [55] for the rest of atoms. This basis set will be denoted as basis2.

To analyze the nature of the bonding, natural bond orbital (NBO) analysis of Weinhold and Carpenter has been used [56]. All B3LYP reported calculations have been carried out with the Gaussian 98 program and are spin unrestricted. CCSD(T) calculations have been done with the MOLPRO 2001 programs system and are spin restricted.

4. Results and discussion

4.1. FAB experiments

Fig. 1 shows the mass spectrum that results from the gas-phase reactions of nickel and chromium ions with formamide. The existence of ^{56}Ni and ^{60}Ni isotopes leads to an easy identification of nickel containing species. The base peak of the spectrum corresponds to the Cr^+ ion at *m/z* 52 and the most abundant Ni containing species is the Ni^+ ion itself at *m/z* 58. The Ni^+ ions react with neutral formamide to produce mainly [Ni–formamide]$^+$ adduct ions at *m/z* 103. This complex can react with another molecule of formamide to produce a small quantity of [Ni(formamide)$_2$]$^+$ complex at *m/z* 148.

The unimolecular decomposition of the [Ni–formamide]$^+$ complex has been investigated by means of the MIKES analysis to obtain information related to the structure and reactivity of this complex ion. The MIKE spectrum is shown in Fig. 2 and shows that the [Ni–formamide]$^+$ ion undergoes several different fragmentations. The major fragmentation corresponds to its dissociation to produce Ni^+ ion at *m/z* 58. The [Ni–formamide]$^+$ shows other losses, namely that of H_2 at *m/z* 101, NH_3 at *m/z* 86 and H_2O at *m/z* 85. Others small peaks are observed at *m/z* 75 and *m/z* 74 that can correspond to the elimination of CO and C, N, H. For comparison, the fragmentation observed in the case of [Cu–formamide]$^+$ system [28], involved the elimination of Cu, H_2O, NH_3, HCO and HCN/CNH but the loss of CO was not observed.

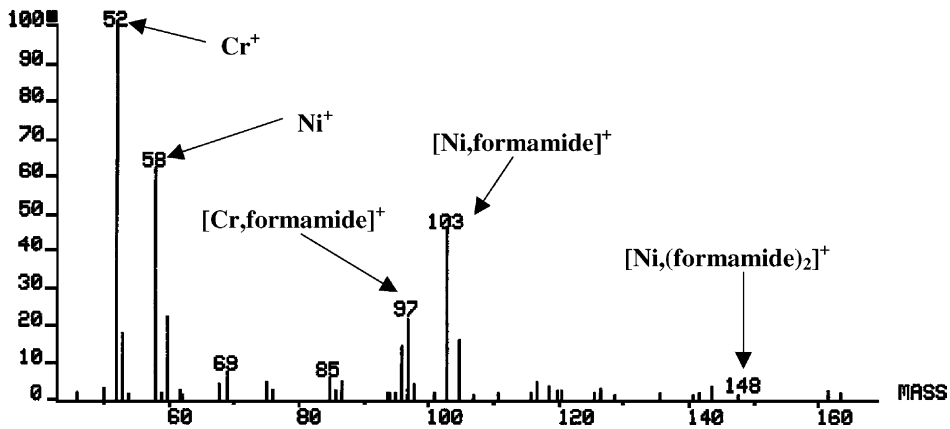

Fig. 1. FAB spectrum that results from the reaction of Ni^+ and Cr^+ sputtered from a foil of an alloy of chromium and nickel, with neutral formamide.

4.2. ESI-MS experiments

At low values of the DP source, spectra of the formamide/$NiSO_4$ aqueous solution show different Ni^+ and Ni^{2+} hydrated complexes (these later species will not be discussed herein). The [Ni–formamide]$^+$ complex only appears at high DPs. Fig. 3 shows the source spectrum at DP = 70 V. As in the case of FAB experiments, nickel containing species are characterized by the presence of two peaks corresponding to ^{58}Ni and ^{60}Ni. Besides the [Ni–formamide]$^+$ ion, several nickel containing adducts can be observed in the source spectrum. The base peak of the spectrum corresponds to *m*/*z* 75. Although we assign this peak to $[NiOH]^+$, the presence of the $[NiNH_3]^+$ ion can not be discarded. The $[NiNH_3]^+$ ion would arise from the decomposition of [Ni–formamide]$^+$ in the source. Other Ni^+ containing species are $[NiOH]^+$, H_2O at *m*/*z* 93 and Ni^+ at *m*/*z* 58. The presence of protonated formamide at *m*/*z* 46 is also observed.

The low energy CID spectrum of selected [Ni–formamide]$^+$ has also been studied. The obtained spectrum recorded at a collision energy of 20 eV is shown in Fig. 4. It can be observed that the most

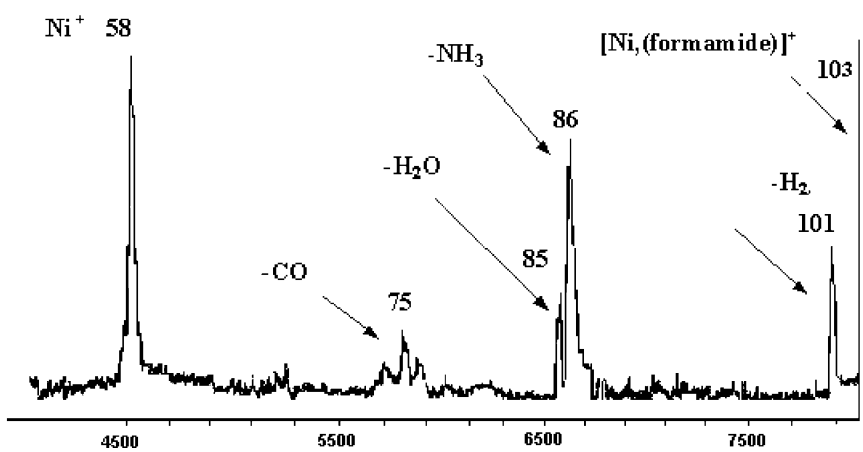

Fig. 2. MIKE spectrum of the [Ni–formamide]$^+$ complex at *m*/*z* 103.

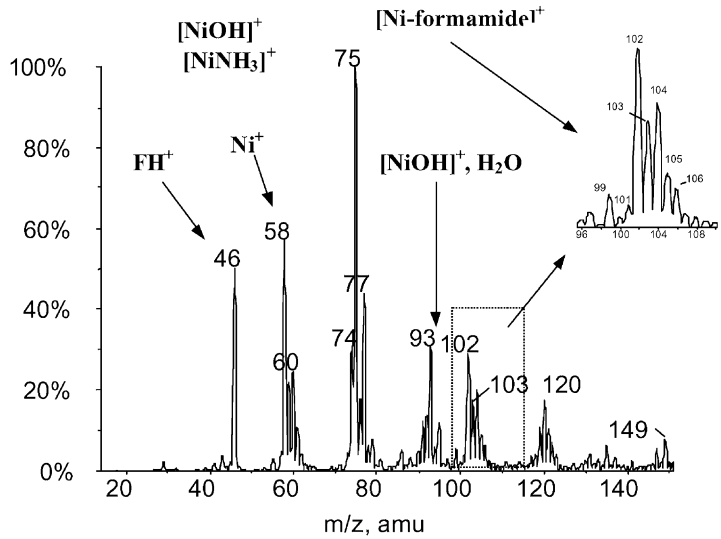

Fig. 3. ESI source spectrum of a solution of formamide and $NiSO_4$ in water solvent. Sampling cone voltage DP = 70 V.

important fragmentation corresponds to the elimination of formamide to produce Ni^+ at *m/z* 58 (base peak of the spectrum). The second most important reaction of the adduct-ion is the elimination of CO at *m/z* 75. Other minor loss corresponds to the elimination of H_2O at *m/z* 85. Thus, it can be observed that the [Ni–formamide]$^+$ ion undergoes fragmentations by different pathways if we use the FAB or the ESI ionization technique.

It should be noted that the peak at *m/z* 103 could be formed in the ESI source by another process. Actually this peak might also arise from the interaction of $[NiOH]^+$ with a CO molecule formed in the decomposition of [Ni–formamide]$^+$. To clarify this point, we have carried out the same ESI-MS/MS study but using ^{15}N labeled formamide. In the source spectrum we obtain the [Ni–(^{15}N)formamide]$^+$ adduct ion at *m/z* 104. The low energy CID spectrum is similar to that

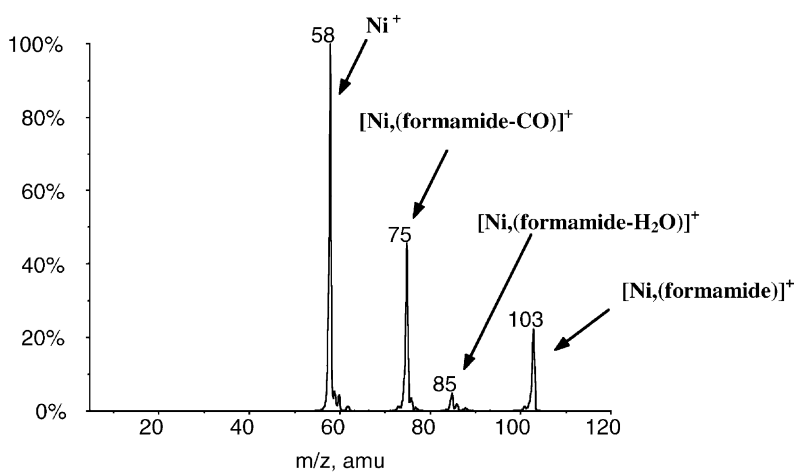

Fig. 4. CID spectrum of [Ni–formamide]$^+$ at *m/z* 103. Sampling cone voltage DP = 70 V and collision energy CE = 20 eV.

obtained previously. Again the base peak of the spectrum corresponds to Ni^+ at *m*/*z* 58. The loss of 28 and 18 units at *m*/*z* 76 and 86 are also observed, thus indicating that in the non labeled experiments the peaks at *m*/*z* 75 and *m*/*z* 103 really correspond to $[NiNH_3]^+$ and [Ni–formamide]$^+$ adduct ions.

To rationalize these experimental findings, we have studied by means of the density functional B3LYP method the most important features of the [Ni–formamide]$^+$ PES. First of all, we have considered the different isomers of [Ni–formamide]$^+$ and second we have explored the possible reaction pathways that lead to the observed fragments.

4.3. Isomers of the [Ni–formamide]$^+$ adduct ion

The relative stability and structure of the different conformers of [Ni–formamide]$^+$ have been studied extensively. We have considered the coordination of Ni^+ to the most stable conformer of formamide ($HCONH_2$) and to its tautomers, i.e., formamidic acid (HN=CHOH) and (aminohydroxy)carbene (H_2N–C–OH). Several of these structures have already been considered in previous studies of protonated or cationized formamide [27,28]. The relative stability of the different tautomers of formamide has been studied previously in our group [27]. We have found that at the G2 level the most stable tautomer is ($HCONH_2$) while (HN=CHOH) and (H_2N–C–OH) lie 11.5 and 37.6 kcal mol^{-1}, respectively above ($HCONH_2$).

Fig. 5 shows the obtained minima for the [Ni–formamide]$^+$ adduct ion. The computed relative energies of the different conformers are shown in Table 1. It can be observed in Fig. 5 that all the structures have C_s symmetry with a $^2A'$ ground state except the **F3** structure which has no symmetry.

The most stable structure (**F1**) corresponds to the metal ion interacting with the oxygen atom of the most stable conformer of formamide, in *trans* with respect to the amino group. The same structure was found to be the most stable in the case of protonated formamide or other cationized formamide systems. The second most stable structure (**F2**) presents the same coordination but with the metal atom in *cis* with respect to the amino group and lies only 2.4 kcal mol^{-1} above at the CCSD(T)/basis1 level. The **F8** and **F9** structures lie 7.5 and 9.7 kcal mol^{-1}, respectively above the most stable one at the CCSD(T)/basis1 level. These two structures correspond to the interaction of Ni^+ with the nitrogen atom of the HN=CHOH tautomer of formamide. The remaining structures corresponding to the association of Ni^+ with the nitrogen atom of formamide (**F3**), oxygen atom of formamidic acid (**F7**) and oxygen and carbon atoms of (aminohydroxy)carbene (**F4**, **F5** and **F6**) lie more than 15 kcal mol^{-1} above the most stable structure (**F1**).

The bonding between formamide and Ni^+ is essentially electrostatic and arises from the interaction of the ^2D (d^9) state of Ni^+ with the $^1A'$ state of formamide. The natural population analysis shows that the metal charge is always larger than 0.75 and the spin density is located in the metal atom (always larger than 0.94). This value of the metal charge indicates that the charge transfer does not have too much influence in the relative stability of the obtained isomers. The relative energies of the different conformers are determined mostly by other factors: the energy difference between the most stable conformer of neutral formamide and the formamide sub-unit in the complex, the electrostatic interaction and the polarization of the formamide moiety due to the presence of the metal cation. Thus, the global minimum (**F1**) corresponds to the Ni^+ cation interacting with the most stable tautomer ($HCONH_2$) of formamide in the direction of the dipolar moment. (The dipole moment of formamide is 4.3 D, the other two enol and cabene tautomers present a dipole moment much smaller: 1.2 and 1.3 D, respectively.) The other structures involving formamide, correspond to less efficient interactions and to geometries of formamide that have lost the planarity (**F3** and **F10**) with the subsequent energy cost.

In the structures involving the second most stable tautomer (HNCHOH) the metal cation interacts with the NH group (**F8** and **F9**). The N atom of this group is more basic and polarizable than the O atom of formamide and thus, the electrostatic interaction in **F8** and **F9** is larger than in **F1**. However, this electrostatic

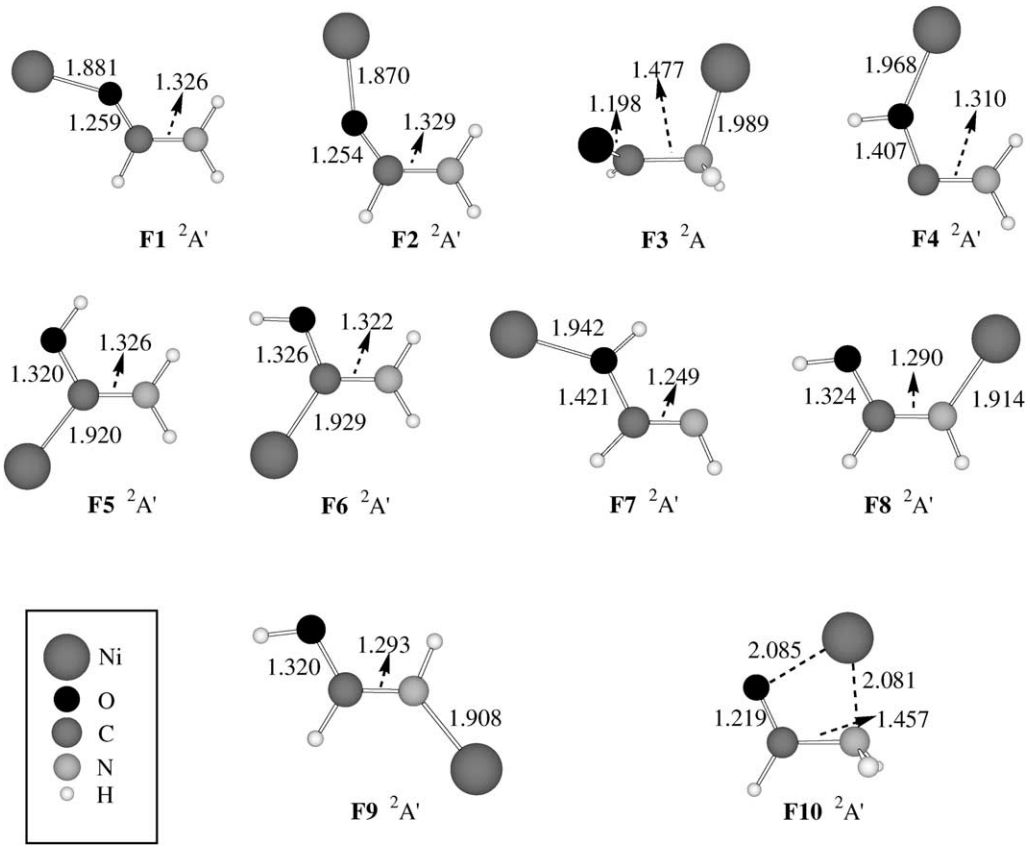

Fig. 5. Optimized geometries for the different minima of the [Ni–formamide]$^+$ complex at the B3LYP/basis1 level. Distances are in Å.

interaction does not compensate the energy difference between the two tautomers of formamide and **F8** and **F9** are 7.5 and 9.7 kcal mol^{-1}, respectively, higher in energy than **F1** at the CCSD(T) level. The **F7** structure also involves the same tautomer but the interaction of Ni^+ with the OH group is much less efficient.

Table 1
Relative energies of the different structures (kcal mol^{-1})

Structure	B3LYP/ basis1	B3LYP/ basis2	CCSD(T)/basis1// B3LYP/basis1
F1	0	0	0
F2	2.2	2.4	2.4
F3	21.5	21.4	18.2
F4	59.2	59.5	57.3
F5	19.0	19.1	23.0
F6	16.8	17.2	21.1
F7	36.4	35.6	32.3
F8	7.8	7.5	7.5
F9	9.5	9.5	9.7
F10	16.1	16.8	12.3

Finally, in structures **F4**, **F5** and **F6** the metal cation interacts with the H_2NCOH carbene. Complexation of Ni^+ to the C atom of this tautomer (**F5** and **F6**) results in a large stabilization due to the high basicity and polarizability of this C atom. However, as in the previous case, this stabilization is not large enough to compensate the energy gap between the formamide tautomers. The **F4** isomer is much less stable than **F5** and **F6** because of the poor interaction of the metal cation with the OH group of the carbene.

In conclusion, the stability order of the tautomers of formamide is reproduced in the complexes but the differences are reduced after complexation because the elctrostatic interaction plus polarization is larger in the complexes involving the HNCHOH and H_2NCOH

tautomers than in the complexes involving the global minimum of formamide, $HCONH_2$.

Table 1 shows that the use of a larger basis set does not produce important changes in the computed B3LYP relative energies of the different conformers. It can also be observed that the B3LYP results are in good agreement with the CCSD(T) ones. The energy ordering is conserved except for the **F3** structure. At the B3LYP level this structure is less stable than **F5** and **F6**, however, at the CCSD(T) level **F3** lies lower in energy than **F5** and **F6**. Nevertheless, these three structures are separated by only 4 or 5 kcal mol^{-1} at the B3LYP or CCSD(T) levels, respectively.

4.4. Binding energies

The binding energies (D_e) of Ni^+–formamide, computed at different levels of calculation are given in Table 2. As it is generally found, the B3LYP binding energies are somewhat overestimated with regard to the ones computed using sophisticated conventional post-Hartre–Fock methods. The difference between the B3LYP and the CCSD(T) methods is 8.5 kcal mol^{-1} using the smaller basis set. This difference is reduced to 6.1 kcal mol^{-1} when augmenting the size of the basis set.

As commented above, the interaction between formamide and Ni^+ is mainly electrostatic. In this kind of metal cation–ligand complex, it is important to describe correctly the dipolar moment and the polarizability of the ligand in order to obtain an accurate description of the interaction energies. Siegbahn and coworkers [57] have shown that the inclusion of diffuse functions in the basis set is necessary to describe properly the dipole moment and the polarizability. Consequently, we need to include diffuse functions to obtain accurate values of the binding energies. In their case, the removal of the diffuse function of the 6-311+G(2d,2p) basis increased the binding energy of $Mg(H_2O)^+$ by 5.7 kcal mol^{-1}. Therefore, in our case the lowering of the binding energy when augmenting the basis set at the B3LYP level is mainly due to the inclusion of the diffuse function in the larger basis set. However, the inclusion of the diffuse function has a small effect in the geometry of the complex as shown by Siegbahn and coworkers [57]. The same trend is observed for the CCSD(T) binding energies. At the CCSD(T) level, the increase of the basis set, usually implies the increase of the binding energy due to the increase of the correlation energy. However, we can observe in Table 2 that the interaction energy of Ni^+–formamide decreases when increasing the basis set. This fact can be attributed to the poor description of the polarizability and the dipole moment of the ligand with the small basis set, as in the case of the B3LYP binding energies. Thus, the lowering of the binding energy associated to the improve in the description of the polarizability and the dipole moment of the ligand when adding the diffuse functions is larger than the increase of the binding energy associated to the increase of the basis set.

Table 2
Interaction Energies (D_e, D_0, ΔH°_{298} and ΔG°_{298}) of Ni^+–formamide (kcal mol^{-1})

	Energy
B3LYP/basis1	66.4
B3LYP/basis2	62.1
CCSD(T)/basis1	57.9
CCSD(T)/basis2	56.0
D_0[a]	54.2
ΔH°_{298}[b]	54.9
ΔG°_{298}[b]	46.9

[a] Determined using the CCSD(T)/basis2 D_e value and the B3LYP/basis1 unscaled harmonic frequencies.

[b] After correction for translational, rotational and vibrational energies determined at the B3LYP/basis1 level.

On the other hand, it should be pointed out that while at the B3LYP level basis2 is large enough to consider the energy converged, regarding the basis set, at the CCSD(T) level the size of this basis could not be sufficient to ensure basis set completion.

The calculated formamide–Ni^+ binding energy (D_e), 56 kcal mol^{-1} at the CCSD(T)/basis2 level and 62.1 kcal mol^{-1} at the B3LYP/basis2 level is slightly larger than the binding energy (D_e) computed for formamide–Cu^+, 53.4 kcal mol^{-1} at the CCSD(T) level reported previously by Hoyau and Ohanessian [58] and 58 kcal mol^{-1} at the B3LYP level by Luna et al. [44]. When the orientation for the interaction of

formamide with both cations are the same (in the direction of one of the oxygen lone pairs) and structures are similar, the Ni–O bond is larger than the Cu–O (1.881 Å vs. 1.845 Å). For the sake of comparison we report the estimated binding energies of formamide toward several other metal cations. The binding energies for formamide–Li^+ and formamide–Na^+ have been estimated to be 46.9 and 33.1 kcal mol^{-1}, respectively at G2(MP2) level [27]. When Mg^+ and Al^+ are concerned, the basicity is enhanced (48.6 and 47.6 kcal mol^{-1}). This enhancement is due to the fact that for these two ions, the interaction is not purely electrostatic, as for alkali cations, but presents a certain covalent character resulting from a dative bond from the oxygen atom to the empty 3p-orbitals of the metal [27]. The association of formamide with Ag^+ has been also quantified and the binding energy was estimated to be 46.8 kcal mol^{-1} [29]. In this case the electrostatic contribution prevails, polarization and charge transfer are less efficient.

4.5. Reactivity of the [Ni–formamide]$^+$ adducts

As mentioned previously, the MIKE and CID spectra of [Ni–formamide]$^+$ shows different fragmentations, namely loss of formamide, H_2, NH_3, H_2O or CO. In this work we have not focused our attention into the H_2 fragmentation. To gain some insight into the mechanisms leading to the rest of the observed fragmentations, we have explored the PES corresponding to some of these processes, which has been schematized in Figs. 6 and 7. In all the reported calculations the energy of the ground state reactants Ni^+ + formamide has been taken as reference. It can be observed that the most favorable route corresponds to the dissociation process into Ni^+ + formamide, in agreement with the experimental observations (see Figs. 2 and 4). Actually, the energy required to dissociate the [Ni–formamide]$^+$ complex is smaller than the activation barriers of the alternative mechanisms.

The two most stable adducts, **F1** and **F2**, are connected by the **TS1** transition state with a barrier of only 3.2 kcal mol^{-1} at the B3LYP/basis2 level. Due to this small interconversion barrier and to the small energy difference between **F1** and **F2**, both adducts have been considered as starting points for the different studied mechanisms. Fig. 6 shows the obtained mechanisms that originates from different hydrogen transfers from the **F1** and **F2** structures. Different reaction paths can be envisaged. In the first case (path I) a 1,2-hydrogen shift from the CH group to the NH_2 group leads from **F1** to the **I2** intermediate through the transition state **TS3** which lies 30.7 kcal mol^{-1} above the reactants Ni^+ + formamide. The resulting **I2** complex is 15.5 kcal mol^{-1} lower in energy that the reactants and corresponds to the NH_3 weakly bound to the carbon atom of $[NiOC]^+$. In this complex the NH_3 moiety can easily dissociate without energy barrier. The 1,2-hydrogen shift in the **F2** isomer (path III) yields the same **I2** product through the transition state **TS5** which is 5.7 kcal mol^{-1} less stable than **TS3**. The third reaction path (II**)** starts with a hydrogen transfer from the CH group to the oxygen of the **F2** structure and leads to **F4** where the metal cation is also attached to the oxygen atom. This step takes place through the transition state **TS2** which is 24.2 kcal mol^{-1} higher in energy than the reactants. The **F4** isomer can easily evolve to **F5** with an activation barrier of 2.6 kcal mol^{-1} through the transition state **TS4**.

Starting from **F5** two different paths are possible. In the first case, the **F5** isomer is connected via **TS7** with a slightly more stable isomer, namely **F6**. The interconversion barrier for this step is 9.2 kcal mol^{-1}. A barrier of 57.2 kcal mol^{-1} (**TS8**) leads from **F6** to **I3,** which corresponds to $[HNC–Ni–H_2O]^+$. This isomer can dissociate into $[NiH_2O]^+$ + HNC or into $[NiCNH]^+ + H_2O$. It should be noted that the loss of H_2O is 20.8 kcal mol^{-1} more favorable than the loss of HNC. This is in agreement with the experimental observations where the peak corresponding to the elimination of HNC is smaller.

The second possibility starting from **F5** involves a transition barrier of 47.2 kcal mol^{-1} (**TS6**) and leads to the global minimum of the PES, **I1**. This isomer corresponds to $[OC–Ni–NH_3]^+$ and could dissociate into $CO + [NiNH_3]^+$ or $NH_3 + [NiCO]^+$, the former being 19.4 kcal mol^{-1} more favorable. However, as shown

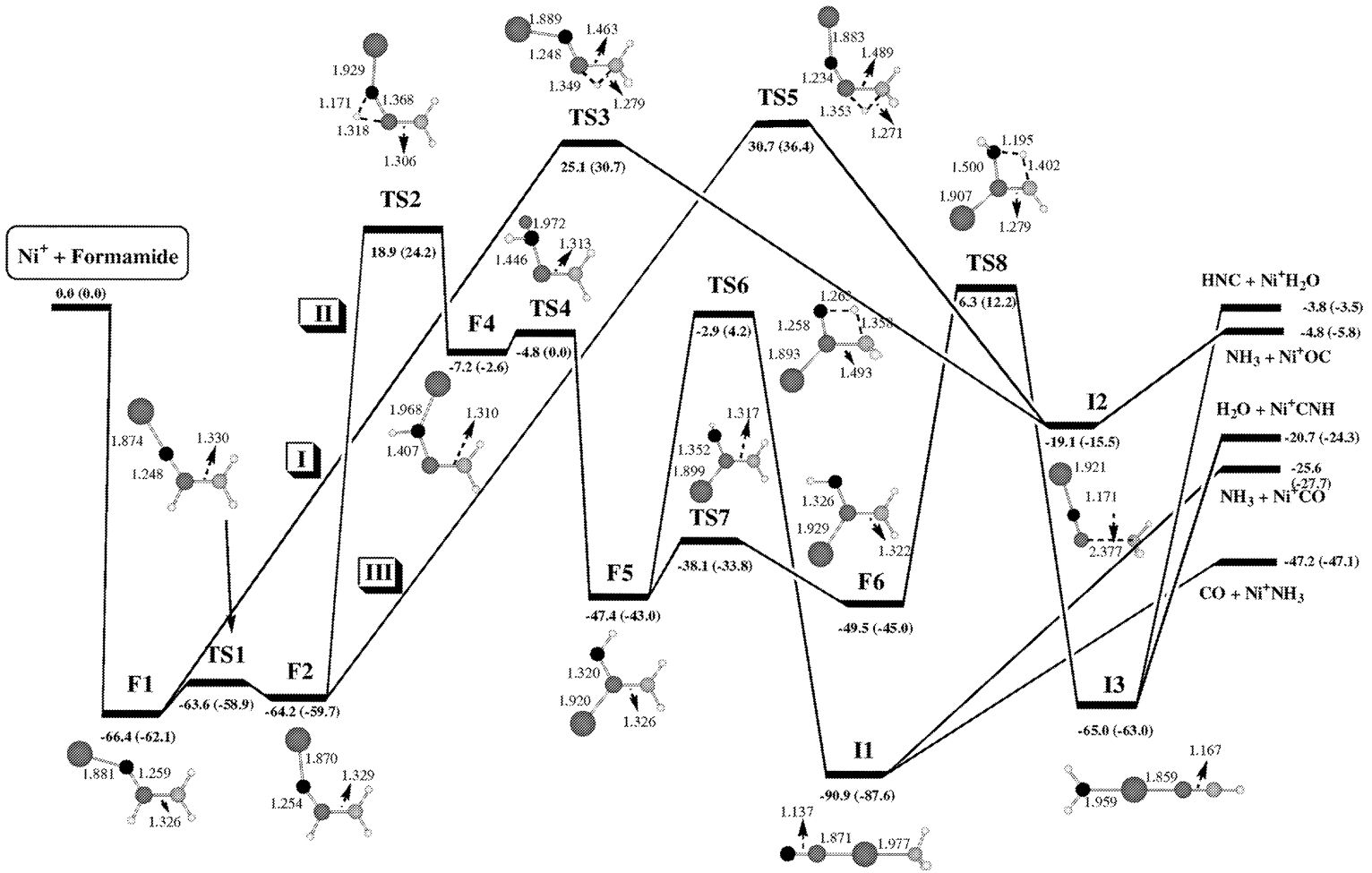

Fig. 6. Schematic representation of the PES associated with several unimolecular reactions of [Ni–formamide]$^+$ starting with a hydrogen transfer in the **F1** and **F2** structures. Distances are in Å and relative energies are in kcal mol^{-1}. Energies computed at the B3LYP/basis2 level are shown in parentheses.

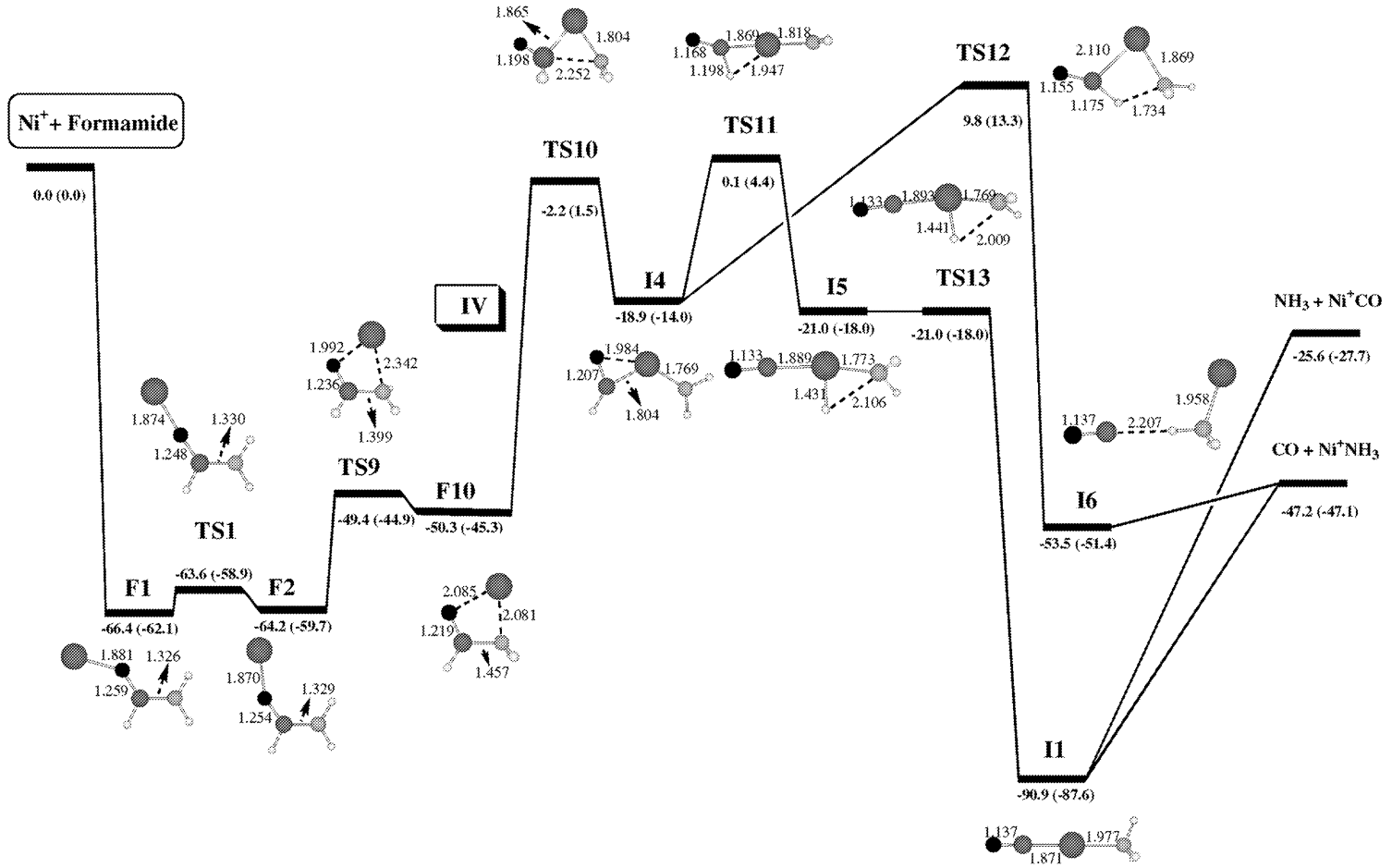

Fig. 7. Schematic representation of the PES associated with several unimolecular reactions of [Ni–formamide]$^+$ starting with the Ni^+ insertion. Distances are in Å and relative energies are in kcal mol^{-1}. Energies computed at the B3LYP/basis2 level are shown in parentheses.

by Luna et al. [28], under FAB collision conditions, the deposition of a large excess of internal energy into the system would favor a direct cleavage of the C–NH_3 bond from **TS6** rather than the reorientation of NH_3 to yield **I1**, which should lead to CO loss.

Fig. 7 shows the mechanism obtained when the Ni^+ metal cation inserts into the C–N bond of formamide (reaction path IV). The transition state **TS9** connects **F2** with **F10** where the metal cation is bound to the oxygen and nitrogen atoms of formamide. The energy barrier for this step is 14.8 kcal mol^{-1}. The insertion of the metal cation into the C–N bond produces the **I4** complex through an energy barrier of 46.8 kcal mol^{-1}. The **I4** structure is 14.0 kcal mol^{-1} more stable than the reactants. This contrasts with the case of $[Cu–formamide]^+$ where all the inserted structures were found to lie above the reactants, and no insertion mechanism was considered. The transition state connecting both minima, **F10** and **I4**, is only 1.5 kcal mol^{-1} higher in energy than the reactants. The **I4** complex corresponds to $[HCO–Ni–NH_2]^+$ and can evolve through two different pathways. The less favorable one involves a direct hydrogen transfer from the HCO moiety to the NH_2 one. This transfer leads to the **I6** complex with a transition barrier of 27.3 kcal mol^{-1} (**TS12**). The **I6** complex corresponds to the CO weakly bound to $[NiNH_3]^+$ and the CO moiety can easily dissociate without barrier in excess. The second possibility involves the transfer of the hydrogen to the metal cation to lead the **I5** complex. In this case **I4** and **I5** are connected by a transition state, **TS11**, which is 4.4 kcal mol^{-1} above the reactants. The **I5** isomer can evolve to **I1** through the transition state **TS13**, which is almost degenerate with **I5**. As in the previous case, **I1** can dissociate into $CO + [NiNH_3]^+$ or $NH_3 + [NiCO]^+$. It should be noted that the **TS13** transition state disappears when optimizing at the B3LYP/basis2 level. In this case, the transition state **TS11** connects the **I4** and **I1** complexes and the minimum **I5** disappears. Actually, an IRC calculation from **TS11** at the B3LYP/basis2 level confirms that this TS connects **I4** and **I1**.

As commented above, the elimination of CO was not observed in the MIKE spectrum of the previously studied $[Cu–formamide]^+$ complex. The main difference between the PESs of both complexes is that for $[Cu\text{-}formaminde]^+$ the insertion mechanism is not favorable. However, in the $[Ni–formamide]^+$ complex this pathway is favorable and leads to the loss of CO.

The experimental results can be explained if one takes into account that the ESI ionization is known to be a 'soft' technique. That is to say, the adduct ions generated by electrospray from solution are less energetically activated that those generated by FAB. In these conditions, the low energy collisional activation that takes place in the CID experiments favors the dissociation through the lower energy pathway. In our case the most energetically favorable pathway is the insertion of the metal cation into the C–N bond which leads to the final loss of CO (pathway IV). However, the internal energy content of the FAB generated ions can be much higher. Moreover, the acceleration voltage applied to the FAB ions (8 kV) is very high compared to the voltage applied in the ESI-CID experiments. In addition, we can not exclude the possibility to have some collisions (in the second field free region) of the adduct ions with the remaining background gas that can induce the deposition of a large excess of internal energy in part of the $[Ni–formamide]^+$ complexes. In these conditions the transfer of a hydrogen atom from the CH group to the NH_2 one and the direct cleavage of the C–NH_3 bond would be favored in front of the other multistep mechanisms.

5. Concluding remarks

Reactions between formamide and Ni^+ in the gas phase under CI-FAB and ESI conditions produce the $[Ni–formamide]^+$ adduct ion. The structure of this ion has been investigated by means of the B3LYP theoretical approach. Several coordinations of Ni^+ to formamide have been considered. The most stable structure corresponds to the interaction of Ni^+ with the oxygen atom in *trans* with respect to the amino group. The estimated Ni^+–formamide D_e binding energy at the CCSD(T) level is 56.0 kcal mol^{-1}.

The reactivity of the [Ni–formamide]$^+$ adduct has been investigated experimentally both, by means of the MIKES analysis and the ESI low energy CID spectrum. Theoretical studies on the reactivity have also been carried out at the B3LYP level. The experimentally observed fragmentations differ depending on the technique used. The MIKE spectrum shows that the major fragmentation of the adduct ion corresponds to the dissociation process to yield Ni^+. The elimination of NH_3 is the second most important reaction. Other losses are observed to a minor extend, namely that of H_2, H_2O, CO and CNH. The low energy ESI-CID spectrum shows that the most important reaction, at a collision energy of 20 eV, also corresponds to the elimination of formamide to produce Ni^+. However, in this case the second most important reaction corresponds to the loss of CO. The elimination of H_2O is also observed.

Theoretical calculations show that all the fragmentations are exothermic regarding to the Ni^+ + formamide reactants. Several pathways leading to the observed fragmentations have been studied. The most favorable process corresponds to the dissociation of the adduct ion into Ni^+ + formamide, as observed experimentally. The pathway leading to the elimination of CO is thermodynamically more favorable than the reaction path leading to the loss of NH_3. This latter reaction is indeed associated with much higher activation barriers. Thus, the low energy collisional activation in the ESI-CID experiments leads to the observation of the loss of CO. However, under FAB conditions, a substantial minority of energetic adducts ions can cross the threshold of dissociation. In these conditions, the direct transfer of the hydrogen of the CH group to the NH_2 group is followed by the cleavage of the C–N bond. This process can be favored in front of the other multistep mechanisms.

Acknowledgements

This work has been partially supported by an allocation of computational time from the Institut de Développement et de Recherche (IDRIS Orsay, France). L.R. acknowledges a postdoctoral Marie Curie grant from the EU.

References

[1] K. Eller, H. Schwarz, Chem. Rev. 91 (1991) 1121.
[2] A. Fontijn (Ed.), Gas-Phase Metal Reactions, North-Holland, Amsterdam, 1992.
[3] B.S. Freiser (Ed.), Organometallic Ion Chemistry, Kluwer Academic Publishers, Dordrecht, 1995.
[4] G.L. Eichhorn, Adv. Inorg. Chem. 3 (1981) 1.
[5] W. Sanger, Principles of Nucleic Acids Structure, Springer, New York, 1984.
[6] R.B. Martin, Acc. Chem. Res. 18 (1985) 32.
[7] H. Sigel, Chem. Soc. Rev. 22 (1993) 255.
[8] V.N. Potaman, V.N. Soyfer, J. Biomol. Struct. Dyn. 11 (1994) 1035.
[9] M. Sabat, B. Lippert, in: A. Sigel, H. Sigel (Eds.), Metal Ions in Biological Systems, Vol. 33, Marcel Dekker, New York, 1996, p. 143.
[10] (a) J. Burda, J. Šponer, P. Hobza, J. Phys. Chem. 100 (1996) 7250;
(b) B.A. Cerda, C. Wesdemiotis, J. Am. Chem. Soc. 118 (1996) 11892;
(c) J. Burda, J. Šponer, J. Leszczynski, P. Hobza, J. Phys. Chem. B 101 (1997) 9670;
(d) J. Šponer, J. Burda, M. Sabat, J. Leszczynski, P. Hobza, J. Phys. Chem. A 102 (1998) 5951;
(e) J. Šponer, M. Sabat, J. Burda, J. Leszczynski, P. Hobza, J. Phys. Chem. B 103 (1993) 2528;
(e) N. Gresh, J. Šponer, J. Phys. Chem. B 103 (1999) 11415;
(f) J. Šponer, M. Sabat, L. Gorb, J. Leszczynski, B. Lippert, P. Hobza, J. Phys. Chem. B 104 (2000) 7535;
(g) C. Fonseca Guerra, M. Bickelhaupt, J.G. Snijders, E.J. Baerends, J. Am. Chem. Soc. 122 (2000) 4117;
(h) M.T. Rodgers, P.B. Armentrout, J. Am. Chem. Soc. 122 (2000) 8548;
(i) J. Muñoz, J. Šponer, P. Hobza, M. Orozco, F.J. Luque, J. Phys. Chem. B 105 (2001) 6051, and references therein.
[11] J.J.R. Faùsto da Silva, R.J.P. Williams, The Inorganic Chemistry of Life, Clarendon Press, Oxford, 1991.
[12] F.W. McLafferty, H.D.R. Schuddenmage, J. Am. Chem. Soc. 62 (1969) 1866.
[13] R.G. Cooks, Collision Spectroscopy, Plenum Press, New York, 1978.
[14] M.W. Senko, J.P. Speir, F.W. McLafferty, Anal. Chem. 66 (1994) 1866.
[15] B.A. Cerda, C. Wesdemiotis, J. Am. Chem. Soc. 117 (1995) 9734.
[16] M.J. Polce, S. Beranova, M.J. Nold, C. Wesdemiotis, J. Mass Spectrom. 31 (1996) 1073.
[17] D. Wen, T. Yalcin, A.G. Harrison, Rapid Commun. Mass Spectrom. 9 (1995) 1155.
[18] T. Yalcin, J. Wang, D. Wen, A.G. Harrison, J. Am. Soc. Mass Spectrom. 8 (1997) 749.

[19] S. Bouchonnet, Y. Hoppiliard, G. Ohanessian, J. Mass Spectrom. 30 (1995) 172.
[20] Q.P. Lei, I.J. Amster, J. Am. Soc. Mass Spectrom. 7 (1996) 722.
[21] H. Lavanant, Y. Hoppiliard, J. Mass Spectrom. 32 (1997) 1037.
[22] H. Lavanant, E. Hecquet, Y. Hoppiliard, Int. J. Mass Spectrom. 185 (1999) 11.
[23] (a) F. Rogalewicz, Y. Hoppiliard, G. Ohanessian, Int. J. Mass Spectrom. 201 (2000) 307;
(b) Y. Hoppiliard, F. Rogalewicz, G. Ohanessian, Int. J. Mass Spectrom. 204 (2000) 267;
(c) F. Rogalewicz, Y. Hoppiliard, G. Ohanessian, Int. J. Mass Spectrom. 206 (2000) 45.
[24] F. Rogalewicz, Y. Hoppiliard, G. Ohanessian, Int. J. Mass Spectrom. 195 (2000) 565.
[25] R.A. Jockusch, A.S. Lemoff, E.R. Williams, J. Am. Chem. Soc. 123 (2001) 12255.
[26] L. Rodríguez-Santiago, M. Sodupe, J. Tortajada, J. Phys. Chem. A 105 (2001) 5340.
[27] J. Tortajada, E. Leon, J.-P. Morizur, A. Luna, O. Mó, M. Yáñez, J. Phys. Chem. 99 (1995) 13890.
[28] A. Luna, B. Amekraz, J. Tortajada, J.-P. Morizur, M. Alcamí, O. Mó, M. Yáñez, J. Am. Chem. Soc. 120 (1998) 5411.
[29] L. Boutreau, E. Leon, A. Luna, P. Toulhoat, J. Tortajada, Chem. Phys. Lett. 338 (2001) 74.
[30] R.G. Cooks, J.H. Beynon, R.M. Caprioli, G.R. Lester, Metastable Ions, Elsevier, New York, 1973.
[31] A.G. Harrison, R.S. Mercer, E.J. Reinee, A.B. Young, R.K. Boyd, R.E. March, C.J. Porter, Int. J. Mass Spectrom. Ion Process. 74 (1986) 13.
[32] R.B. Freas, M.M. Ross, J.E. Campana, J. Am. Chem. Soc. 107 (1985) 6195.
[33] G. Hornung, D. Schröder, H. Schwarz, J. Am. Chem. Soc. 117 (1995) 8192.
[34] (a) A.D. Becke, J. Chem. Phys. 98 (1993) 5648;
(b) C. Lee, W. Yang, R.G. Parr, Phys. Rev. B 37 (1988) 785;
(c) P.J. Stevens, F.J. Devlin, C.F. Chablowski, M.J. Frisch, J. Phys. Chem. 98 (1994) 11623.
[35] M.C. Holthausen, C. Heineman, H.H. Cornehl, W. Koch, H. Schwarz, J. Chem. Phys. 102 (1995) 4931.
[36] C. Adamo, F. Lelj, J. Chem. Phys. 103 (1995) 10605.
[37] M.R.A. Blomberg, P.E.M. Siegbahn, M. Svensson, J.Chem. Phys. 104 (1996) 9546.
[38] L. Rodríguez-Santiago, M. Sodupe, V. Branchadell, J. Chem. Phys. 105 (1996) 9966.
[39] (a) A. Ricca, C.W. Bauschlicher, J. Phys. Chem. 98 (1994) 12899;
(b) C.W. Bauschlicher, P. Maitre, J. Phys. Chem. 99 (1995) 3444;
(c) A. Ricca, C.W. Bauschlicher, Theor. Chim. Acta 92 (1995) 123.
[40] A. Irigoras, O. Elizalde, I. Silanes, J.E. Fowler, J. Ugalde, J. Am. Chem. Soc. 122 (2000) 114.
[41] C.W. Bauschlicher, A. Ricca, H. Partridge, S.R. Langhoff, in: D.P. Chong (Ed.), Recent Advances in Density Functional Theory, Part II, World Scientific, Singapore, 1997, p. 38.
[42] A. Luna, B. Amekraz, J.-P. Morizur, J. Tortajada, O. Mo, M. Yañez, J. Phys. Chem. 101 (1997) 5931.
[43] J. Bertran, L. Rodriguez-Santiago, M. Sodupe, J. Phys.Chem. B 103 (1999) 2310.
[44] A. Luna, B. Amekraz, J. Tortajada, Chem. Phys. Lett. 31 (1997) 31.
[45] T. Marino, N. Russo, N. Toscan, J. Inorg. Biol. 79 (2000) 179.
[46] S. Pulkkinen, M. Noguera, L. Rodríguez-Santiago, M. Sodupe, J. Bertran, Chem. Eur. J. 6 (2000) 4393.
[47] A. Luna, M. Alcamí, O. Mo, M. Yañez, Chem. Phys. Lett. 320 (2000) 129.
[48] S. Hoyau, G. Ohanessian, J. Am. Chem. Soc. 119 (1997) 2016.
[49] S.S. Yi, M.R.A. Blomberg, P.E.M. Siegbahn, J.C. Weisshaar, J. Phys. Chem. A 102 (1998) 395.
[50] A.J.H. Wachters, J. Chem. Phys. 52 (1970) 1033.
[51] P.J. Hay, J. Chem. Phys. 66 (1977) 4377.
[52] T.H. Dunning, J. Chem. Phys. 53 (1970) 2823.
[53] M.J. Frisch, G.W. Trucks, H.B. Schlegel, G.E. Scuseria, M.A. Robb, J.R. Cheeseman, V.G. Zakrzewski, J.A. Montgomery Jr., R.E. Stratmann, J.C. Burant, S. Dapprich, J.M. Millam, A.D. Daniels, K.N. Kudin, M.C. Strain, O. Farkas, J. Tomasi, V. Barone, M. Cossi, R. Cammi, B. Mennucci, C. Pomelli, C. Adamo, S. Clifford, J. Ochterski, G.A. Petersson, P.Y. Ayala, Q. Cui, K. Morokuma, D.K. Malick, A.D. Rabuck, K. Raghavachari, J.B. Foresman, J. Cioslowski, J.V. Ortiz, A.G. Baboul, B.B. Stefanov, G. Liu, A. Liashenko, P. Piskorz, I. Komaromi, R. Gomperts, R.L. Martin, D.J. Fox, T. Keith, M.A. Al-Laham, C.Y. Peng, A. Nanayakkara, C. Gonzalez, M. Challacombe, P.M.W. Gill, B. Johnson, W. Chen, M.W. Wong, J.L. Andres, C. Gonzalez, M. Head-Gordon, E.S. Replogle, J.A. Pople, Gaussian 98, Revision A.7, Gaussian, Inc., Pittsburgh, PA, 1998.
[54] C.W. Bauschlicher Jr., S.R. Langhoff, L.A. Barnes, J. Chem. Phys. 91 (1989) 2399.
[55] R. Krishnan, J.S. Binkley, R. Seeger, J.A. Pople, J. Chem. Phys. 72 (1980) 650.
[56] (a) F. Weinhold, J.E. Carpenter, The Structure of Small Molecules and Ions, Plenum Press, New York, 1988;
(b) A.E. Reed, L.A. Curtiss, F. Weinhold, Chem. Rev. 88 (1988) 899.
[57] M. Pavlov, P.E.M. Siegbahn, M. Sandström, J. Phys. Chem. A. 102 (1998) 219.
[58] S. Hoyau, G. Ohanessian, Chem. Phys. Lett. 280 (1997) 266.